

U. S. DEPARTMENT OF COMMERCE  
NATIONAL OCEANIC AND ATMOSPHERIC ADMINISTRATION  
NATIONAL WEATHER SERVICE  
NATIONAL METEOROLOGICAL CENTER

OFFICE NOTE 77

On the Feasibility of Integrating  
a Combined LFM-PBL Model

J. Gerrity, E. Gross, and R. McPherson  
Development Division

JUNE 1972

## 1. Introduction

In September 1971, an effort was undertaken at the National Meteorological Center (NMC) to examine the feasibility of combining the U.S. Air Force Global Weather Central's (GWC) planetary boundary layer (PBL) model with the NMC limited-area fine-mesh (LFM) primitive equation model. For approximately three years, GWC has been utilizing the PBL model as a part of its operational numerical forecasting system (Hadeen, 1970). At GWC, the PBL model is used in conjunction with a six-level fine-mesh filtered equation forecast model (Howcroft, 1966). The recent implementation of the NMC LFM model (Howcroft and Desmarais, 1972) provided the basic dynamical framework for implementation of the dynamically passive GWC PBL model (Gerrity, 1967) at NMC.

The feasibility test reported here required the development of an objective analysis code suitable for processing surface and upper air observations into the initial data required by the PBL model. Additional coding was needed to derive the boundary conditions required to drive the PBL model. These conditions are obtained in part from the history tape generated by the LFM forecast model and in part from topological and climatological data for the geographic region comprising the PBL integration domain (cf. Fig. 1).

Another major component of the effort involved the modification and debugging of the PBL forecast code for the NMC computing system. An annotated listing of the PBL code and a card deck were kindly made available to us by GWC personnel. A similar contribution was also made by personnel of Drexel University who were studying the GWC model under a government contract.

The final major component of the project was the development of graphics for displaying the model forecasts in suitable formats. This work was greatly eased through the acquisition by the NOAA Computer Division of a microfilm output device. The personnel of the Computer Division assisted in the design of the background charts for map displays and provided technical guidance in utilizing the equipment.

Detailed descriptions of each of the three aforementioned efforts have been documented (Gross, Jones, and McPherson, 1972). The information contained therein will prove to be valuable to prospective users of the analysis-prediction package.

In the present report, we shall present some results obtained with the new model in order to illustrate the technical feasibility of its implementation at NMC. The applicability of the model to aviation and severe weather prediction will be indicated. The results presented here are not regarded as demonstrations that the model has been optimized. They are regarded rather as indications that the model has sufficient promise to warrant further test and evaluation. Possible improvements in the analysis and prediction package have been indicated by Gross, Jones and McPherson (op. cit.).

## 2. Background Information

It is beyond the scope of this paper to discuss the details of the analysis and prediction models utilized to obtain the forecast material presented subsequently. The interested reader should refer to the references indicated in the Introduction. One must, however, recognize certain fundamental facts in order to appreciate the material which is presented.

The basic dynamics of the forecast system are provided by the LFM model through the horizontal wind field predicted by that model at the 1600 m level above the ground. That wind field is assumed to be approximately geostrophic for the purpose of providing an upper boundary condition for the boundary layer wind field. The details of the wind profile in the boundary layer are based on the existence of an Ekman spiral modified by a mean thermal wind between 1600 m and 50 m above the ground. The vertical eddy flux of momentum and the wind direction at the 50 m level are also imposed as lower boundary conditions for the horizontal wind diagnostic equation. These quantities are calculated by the PBL model.

The PBL model is therefore dependent upon the LFM model for the accurate prediction of the circulation at 1600 m above the ground and for the basic horizontal pressure force acting through its depth. The thermal field within the PBL is however entirely predicted by the PBL model. The prediction of wind hodographs that are far from spiral in form can be attributed to the baroclinicity of the boundary layer predicted by the PBL model.

The temperature field predicted by the PBL model is influenced near the ground by climatologically derived radiation effects modified by the presence of clouds. The cloudiness is predicted at upper levels by the LFM and at lower levels by the PBL model. A surface based diurnal temperature oscillation is observed in the forecasts, although it may sometimes be modified in reality by the cooling of the ground surface by strong cold outbreaks, a process not incorporated in the PBL model.

Although the wind field is calculated using a constant eddy viscosity in the transition, or Ekman layer, the temperature and water vapor are vertically diffused using a stability dependent exchange coefficient. The temperature and moisture profiles predicted by the model may therefore have some skill in maintaining or forming elevated inversions.

The vertical structure of the PBL model is shown in Figure 2. It will be noted that the coordinate surfaces follow the elevation of the ground. In the western United States, the mountainous terrain poses serious modeling difficulties. The prediction model was not designed to treat local

circulations which may dominate the low-level meteorological profiles in such environments. The model's forecasts are valid on the so-called "sub-synoptic" scale and are not properly thought of as mesoscale forecasts. In spite of this fact, one may find the small-synoptic-scale forecasts to be of considerable assistance in the specification of the probability of occurrence of mesoscale phenomena.

Finally, it should be noted that the PBL model does not influence the LFM forecast. The LFM model uses a formulation of the boundary layer based on a very limited vertical resolution and relatively simple bulk formulas for frictional drag and sensible heat transfer. Although it is true that the boundary layer processes can have an influence upon the dynamics of the free air, the general scientific consensus is that this influence is generally a slow cumulative process. In special circumstances, such as when a tropical storm makes a landfall, a sudden and dynamically significant interaction takes place. The future possibility of constructing a detailed combined model may prove to be useful in such cases and is probably desirable for extended range forecast applications. The PBL model presently in hand is intended as an interim measure to provide detailed guidance for shorter range weather forecasts.

### 3. Sample Forecasts

In order to provide a basis for determining the feasibility of integrating the new LFM-PBL analysis-prediction model in the NMC environment and in order to obtain a qualitative assessment of the model's performance, several semi-real time calculations were made.

Detailed synoptic case studies were not carried out and for this reason the presentation will not enter into an evaluation of the accuracy of the forecasts. It may be noted, however, that the model provides forecast detail - the accuracy of which will be difficult to assess by reason of the sparsity of observational data coverage on the predicted scales.

#### 3.1 Case: 00Z February 19, 1972

The observed surface maps for this case are shown in figures 3a, 4a, and 5a. The wind predicted for the 50 m level by the combined LFM-PBL model is shown in figures 3b, 4b and 5b. The winds are plotted using conventional symbols at each gridpoint. Also shown are the isopleths of predicted surface temperature at intervals of 10°F. One should recall that the development of the circulation is largely controlled by the LFM forecast through the imposed upper boundary condition. The unreasonable winds shown over Mexico are probably related to the rough orographic configuration in that area and to deficiencies in the analysis and modeling scheme for such regions. In this synoptic situation, the proximity of the eastern boundary of the PBL grid to the active development is responsible for relatively large errors in the predicted temperature field to the east of the storm.

Figures 6a, 7a and 8a display the weather depiction charts for this case. Regions of low cloudiness and precipitation are noted by scalloping. A heavy dashed line is entered to indicate the separation between rainfall and snow. The mean relative humidity predicted in the boundary layer is shown in Figures 6b, 7b and 8b. A dashed line delineates the separation between areas in which the boundary layer temperatures were predicted to be above freezing and those areas in which at least part of the boundary layer was at temperatures below freezing.

This sort of vertically integrated depiction chart does not lend itself to adequate presentation of the forecast information. Figures 9, 10 and 11 are time cross sections of the forecasts at gridpoints near three major cities. The wind, temperature and relative humidity are plotted at each model level at each hour. Solid contours are drawn at intervals of 1°C. The relative humidity is isoplethted at 10% intervals using dashed lines. The predicted surface temperature is given in degrees Fahrenheit along the base of the figure. Along the top of the figure the hourly surface observations are presented.

One must await objective verification of the accuracy of these forecasts. It does seem that this method of presenting the predictions would be useful to field station forecasters especially in timing the onset of significant changes in local conditions.

To permit a qualitative assessment of the accuracy of these time sections, the observed radiosonde data at these stations is shown in figures 12, 13, and 14.

### 3.2 Case 12Z May 2, 1972

During this 24 hr period, a slowly filling low moved from eastern Iowa to Lake Huron. To the southeast of the low, widespread thunderstorm activity was observed to occur in advance of a slowly moving cold front. During the period 21Z to 01Z, tornadoes were reported<sup>1</sup> as follows:

15 mi. NNW of Brownsville, Tex.	at 21Z
15 mi. SE of Buffalo, N. Y.	at 23Z
36 mi. SE of McComb, Miss.	at 01Z
25 mi. NE of Youngstown, Ohio	at 01Z

---

<sup>1</sup> Information provided by Dr. Bonner of TDL.

The synoptic situation is displayed in Figures 15, 16 and 17. The sea level isobars and surface frontal analyses are shown together with reported surface weather and nearly synoptic radar summaries.

Figures 18, 19 and 20 were prepared from the LFM-PBL model forecast data. The wind forecast at 50 m is plotted in standard form at each grid point. The solid contours are isopleths of the "best lifted index" (BLI) parameter (Fujita, 1970). These values were derived by scanning the several vertical levels at which temperature and dewpoint temperature are predicted by the PBL model. Each point was then "lifted" pseudo-adiabatically to 500 mb and the temperature of the parcel compared with the 500 mb temperature predicted by the LFM model. The most unstable index was chosen and the pressure of the parcel prior to lifting was noted. The pressures were obtained through interpolation from LFM model forecasts. According to Dr. Bonner of TDL, severe thunderstorms are expected to occur in conjunction with a combination of large negative BLI's and low values of the pressure of the parcel prior to lifting.

#### 4. Summary and Recommendations

This report has presented results of the effort to implement the Air Force PBL model in conjunction with the LFM model at the NMC. In its present stage of development, the LFM-PBL package has been shown to function in broad agreement with our expectations.

There are a number of further development efforts which might be undertaken with this combined model. The code may be rewritten to function more efficiently in the operational cycle. As presently configured, the entire package requires approximately thirteen minutes of CDC 6600 CPU time and a very large amount of core.

The results obtained to date suggest that the prediction and analysis schemes may be improved upon by further experimental effort. On the other hand, if the present model formulation is found useful, it may be wise to delay further experimental efforts until the principal deficiencies of the model have been identified through operational experience.

Perhaps the most difficult questions involve the determination of the best methods for disseminating the forecast information to potential users and to involving them in an evaluation of the utility of the guidance material.

A decision on a course to be followed ought to involve NMC, TDL and representatives of one or more of the regions. As presently configured, one would think that the model forecasts would be most useful in the Central Region.

## 5. Acknowledgments

The assistance of many groups and individuals require acknowledgment. Professor Kreitzberg and his colleagues at Drexel University provided us with copies of the GWC model and some test cases. Drs. Alaka, Bonner and Long of TDL helped to formulate the objectives of this effort. Major Flattery and Captain Goddard of Air Weather Service assisted in the project and provided liaison with the Global Weather Central. Several of our colleagues at NMC, especially Mr. Howcroft, generously assisted in various stages of the effort. Mrs. Duane Kidwell of the NOAA Computer Division provided expertise in the design of graphical depictions.

## 6. References

- Fujita, T. T., et al., 1970: "Palm Sunday Tornadoes of April 11, 1965," Monthly Weather Review, 98:1, pp. 29-69.
- Gerrity, J. P., Jr., 1967: "A Physical-Numerical Model for the Prediction of Synoptic-Scale Low Cloudiness," Monthly Weather Review, 96(5), May, 261-282.
- Gross, E., R. Jones, and R. McPherson, 1972: "A Description of the NMC Planetary Boundary Layer Model," NMC Office Note 75, Development Division, National Meteorological Center, Suitland, Maryland.
- Hadeen, K. D., 1970: "AFGWC Boundary Layer Model," AFGWC Tech. Memo. 70-5, Air Weather Service, Offut AFB, Nebraska.
- Howcroft, J. G., 1966: "Fine-Mesh, Limited-Area Forecasting Model," Tech. Report 188, Air Weather Service, Scott AFB, Illinois.
- Howcroft, J. G., and A. Desmarais, 1972: "An Operational Limited-Area Fine-Mesh Forecasting Model." (Manuscript to be submitted for publication)

Captions for Figures:

- Figure 1. A polar stereographic map of the Northern Hemisphere, showing the region of integration of the PBL model, innermost rectangle, and of the LFM model, the larger rectangle. The octagon encloses the region for which objective analyses are routinely made at NMC. The mesh size used in the integrations is shown in one corner of the LFM region.
- Figure 2. A schematic representation of the vertical structure of the PBL model. Note that the vertical coordinate surfaces follow the shape of the underlying terrain.
- Figure 3. (A) Surface chart analysis for 00Z 19 February 1972.  
(B) Diagnosed 50 m wind field plotted using the convectional arrow and barb scheme. Analyzed surface temperature isopleth at 10°F intervals.
- Figure 4. (A) Surface chart analysis for 12Z 19 February 1972.  
(B) Predicted 50 m wind field and surface isotherms valid at 12Z 19 February 1972.
- Figure 5. (A) Surface chart analysis for 00Z 20 February 1972.  
(B) Predicted 50 m wind field and surface isotherms valid at 00Z 20 February 1972.
- Figure 6. (A) Weather depiction chart for 0100Z 19 February 1972. Dashed line separates rain from snow.  
(B) Isopleths of the mean relative humidity analyzed in the lowest 1600 m above the ground at 00Z 19 February 1972. The dashed line shows separation between moist areas in which the PBL temperature is entirely above freezing and those in which part of the PBL is below freezing.
- Figure 7. (A) Weather depiction chart for 1300Z 19 February 1972. Dashed line separates rain from snow.  
(B) Isopleths of the mean relative humidity predicted by the PBL model, valid at 1200Z 19 February 1972. The dashed line separates moist areas within which the PBL model predicted temperatures above freezing throughout the lowest 1600 m from those within which part of that layer was forecast to be below freezing.
- Figure 8. (A) Same as Fig. 7 except times 0100Z 20 February 1972.  
(B) Same as Fig. 7 except times 0000Z 20 February 1972.

Figure 9. Time cross section for Nashville predicted by the PBL model. Initial time is 00Z 19 February 1972. Winds are plotted using conventional arrows and barbs. Temperature is isoplethted with solid curves at intervals of 1°C. Relative humidity is isoplethted with dashed curves at intervals of 10%. The predicted surface temperature is given in degrees Fahrenheit along the base of the figure. The hourly observations of surface weather are indicated along the top of the figure.

Figure 10. The same as Fig. 9 but for New York City.

Figure 11. The same as Fig. 9 but for Washington, D.C.

Figure 12. (A) Rawinsonde observation for Nashville at 12Z 19 February 1972.  
(B) Rawinsonde observation for Nashville at 00Z 20 February 1972.  
Solid line - Temperature      Dashed line - Dewpoint

Figure 13. (A) Same as Fig. 12, except  
(B) for Kennedy Airport, N.Y.

Figure 14. (A) Same as Fig. 12, except for  
(B) Dulles International Airport.

Figure 15. Sea level isobars and surface frontal analysis together with nearly synoptic radar summaries and reported surface weather for 12Z 2 May 1972.

Figure 16. Same as Fig. 15, except for 00Z 3 May 1972.

Figure 17. Same as Fig. 15, except for 12Z 3 May 1972.

Figure 18. Diagnosed 50 m winds, Best Lifted Index (solid curves) and pressure of BLI (dashed curves) in mb for 12Z 2 May 1972.

Figure 19. Predicted 50 m winds, Best Lifted Index (solid curves) and pressure of BLI (dashed curves) in mb for 00Z 3 May 1972.

Figure 20. Same as Fig. 19 but for 12Z 3 May 1972.

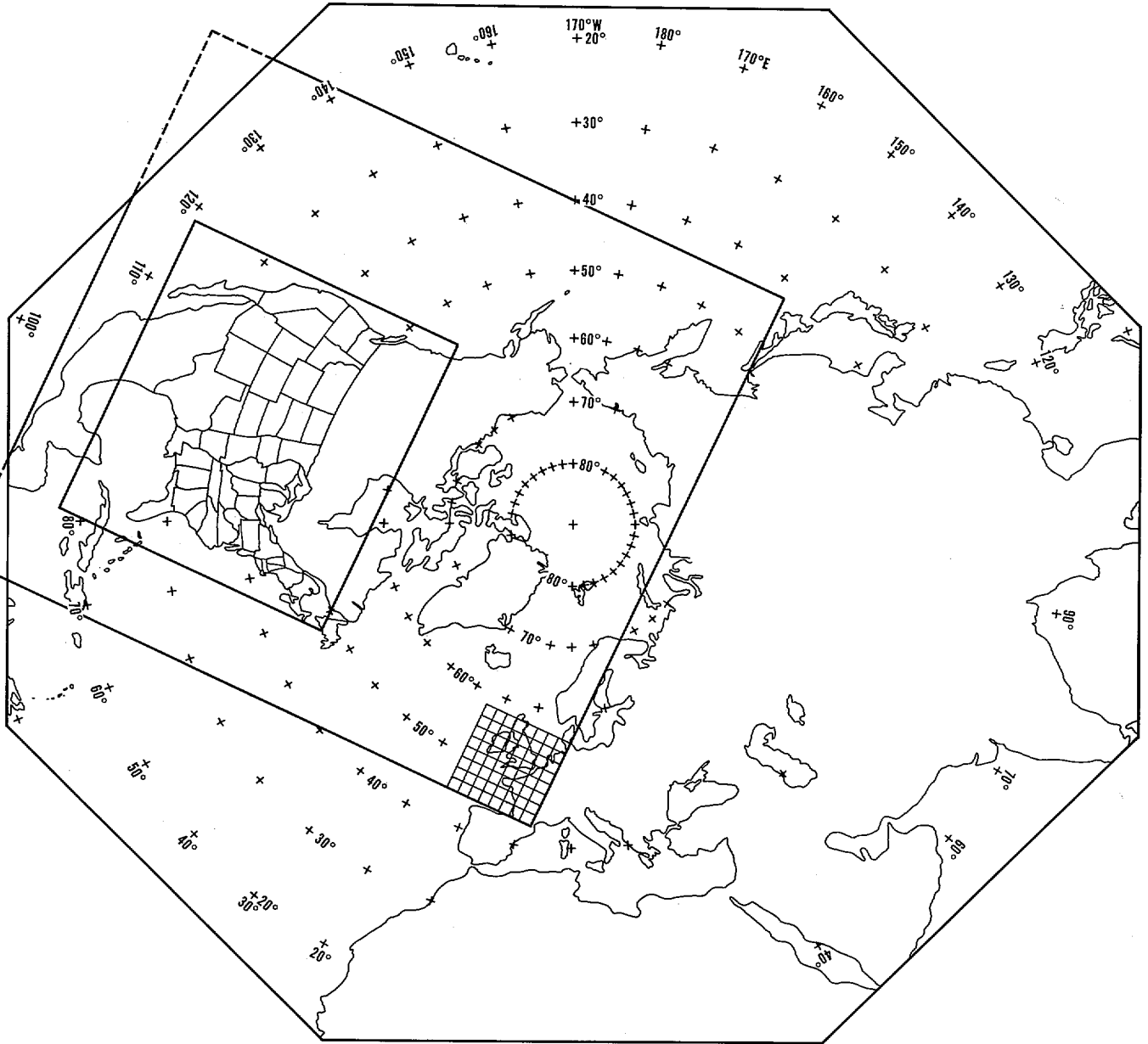


Figure 1.



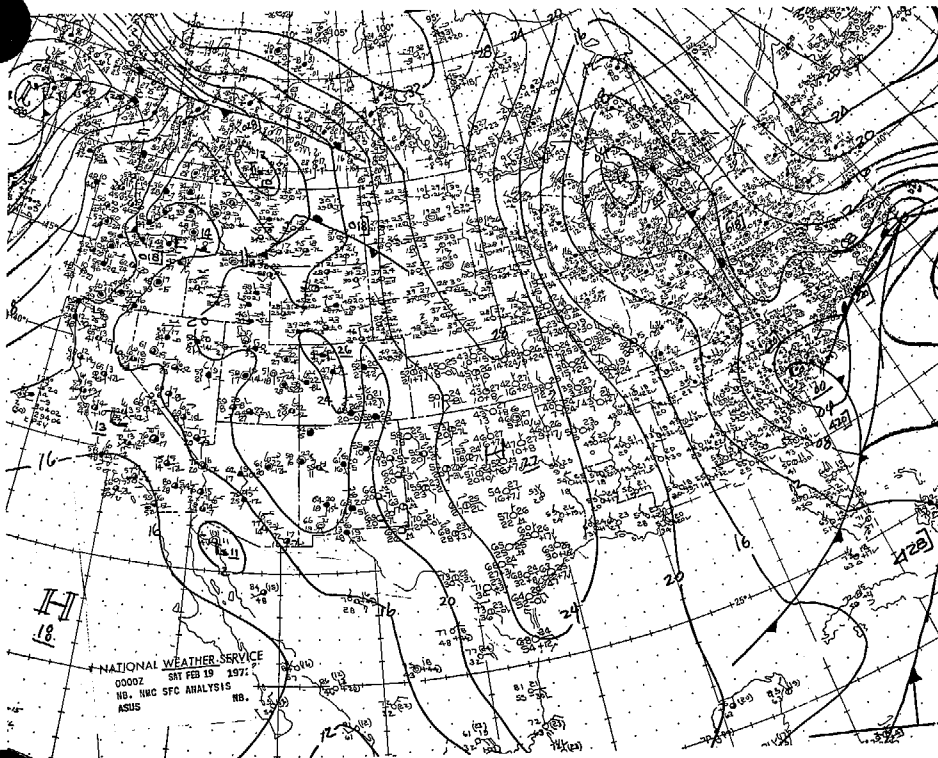
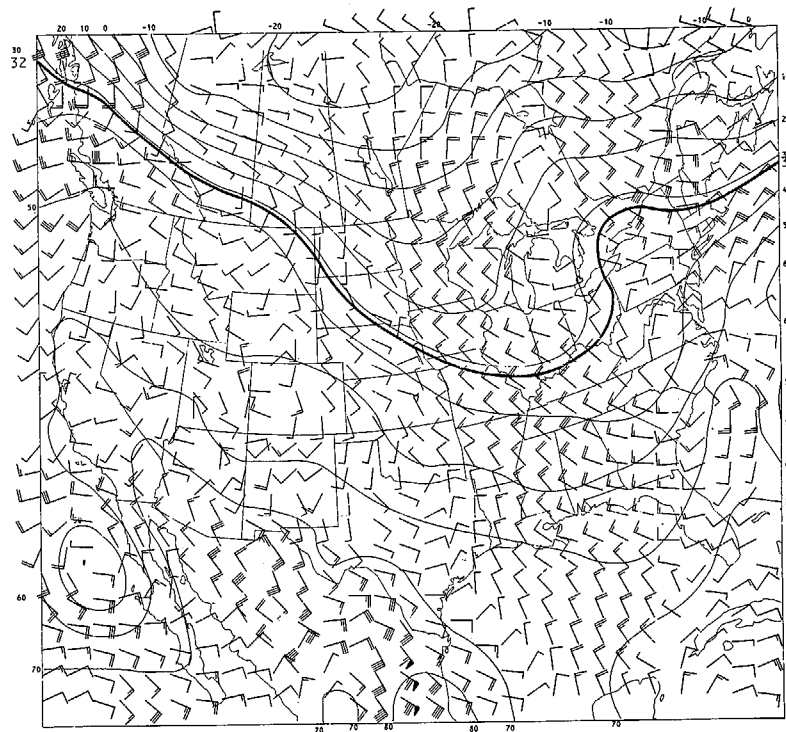


Figure 3(A)



50 METER WIND AND SURFACE TEMP FCST V.T. 0 HRS AFTER 00Z 19/ 2/72

Figure 3(B)

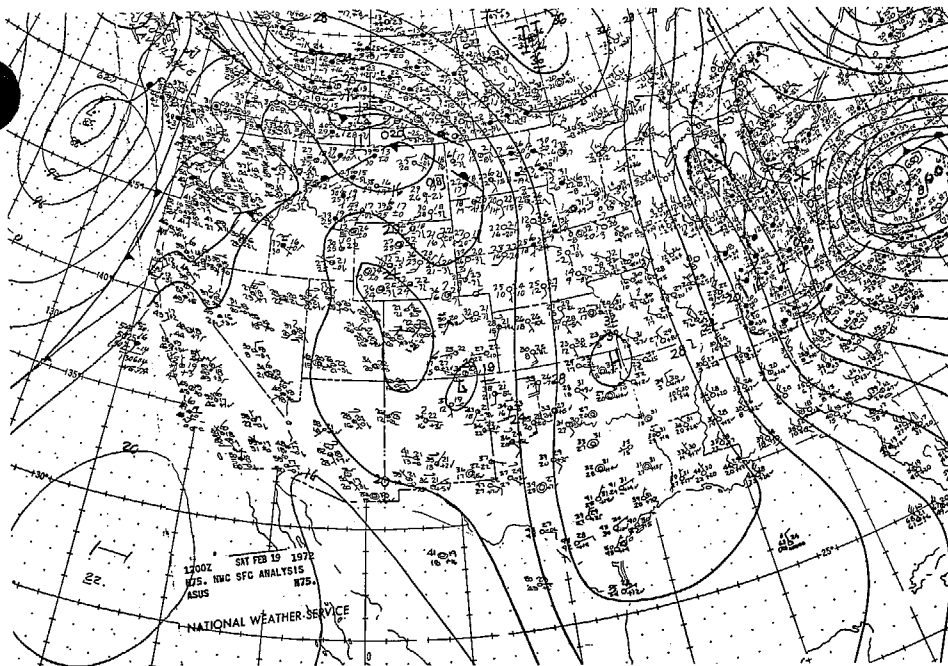


Figure 4(A)

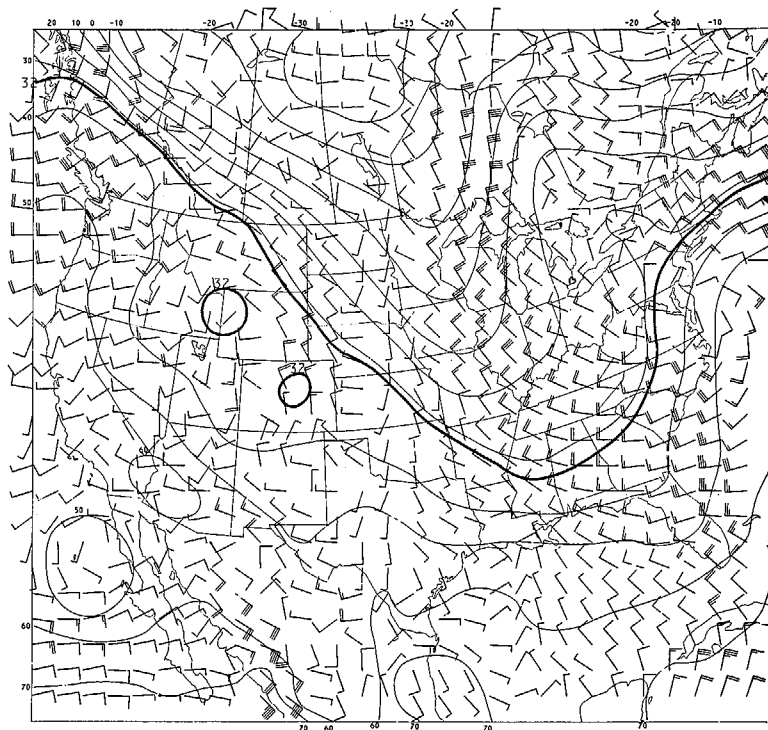


Figure 4(B)

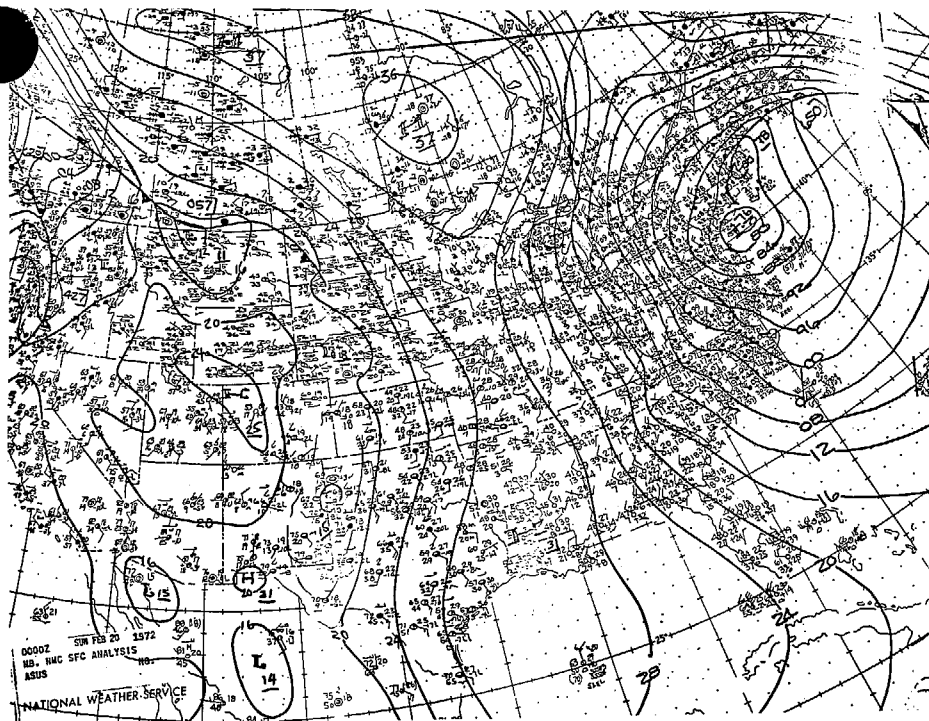
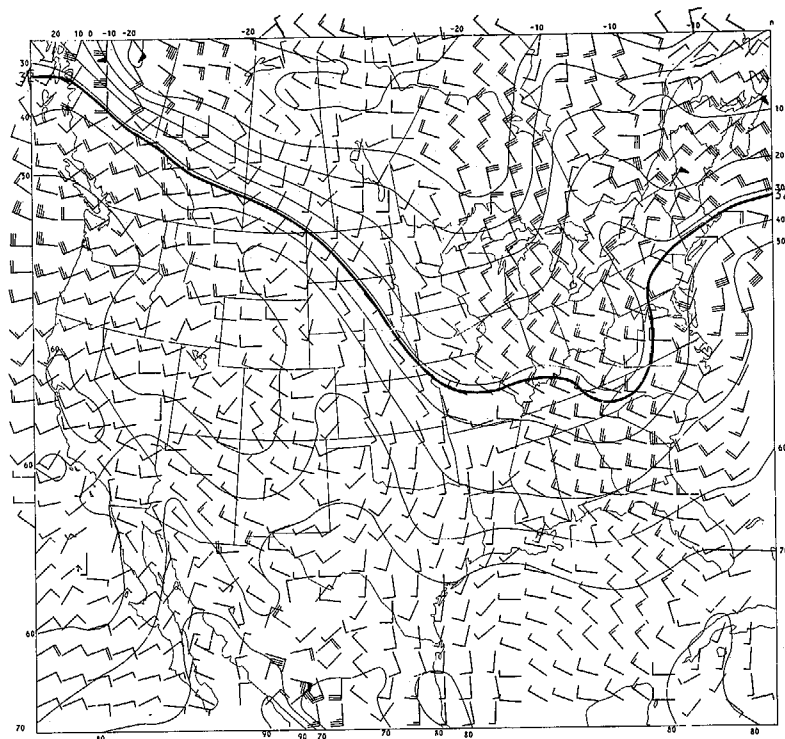
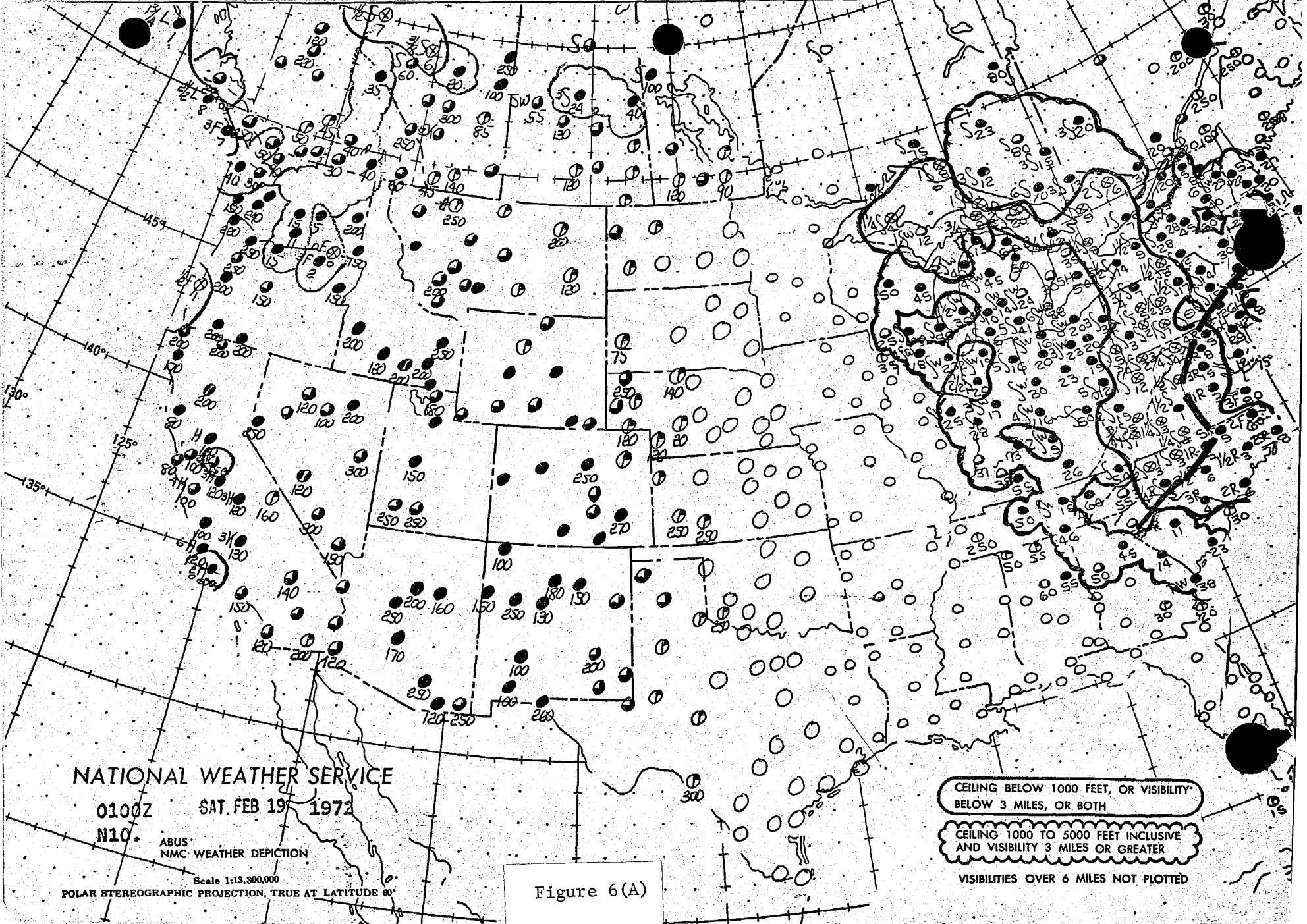


Figure 5(A)



50 METER WIND AND SURFACE TEMP FCST V.T. 24 HRS AFTER 00Z 19/ 2/72

Figure 5(B)



NATIONAL WEATHER SERVICE

0100Z SAT. FEB 19 1972

N10  
 ABUS  
 NMC WEATHER DEPICTION

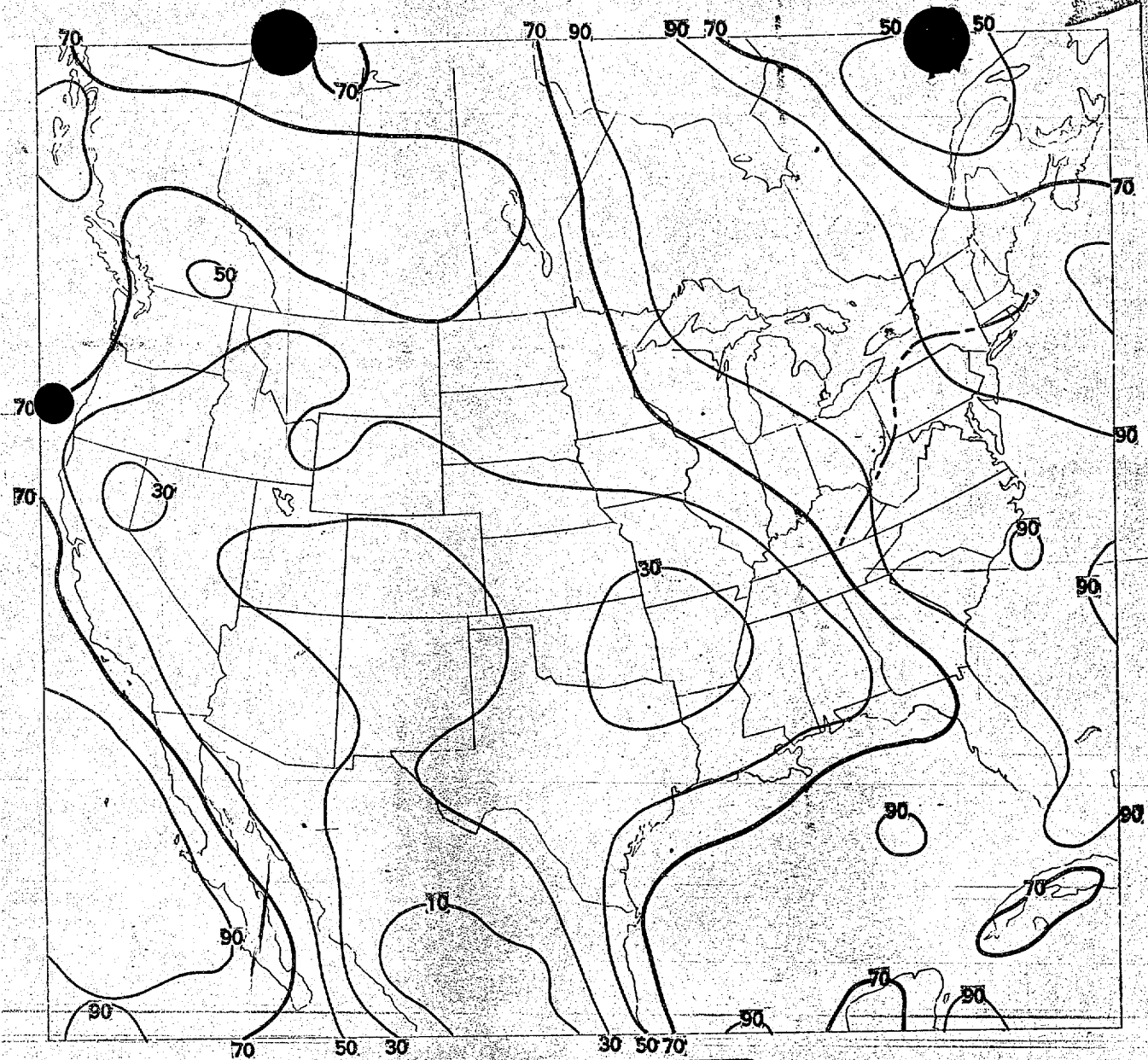
Scale 1:13,300,000  
 POLAR STEREOGRAPHIC PROJECTION, TRUE AT LATITUDE 80°

Figure 6(A)

CEILING BELOW 1000 FEET, OR VISIBILITY  
 BELOW 3 MILES, OR BOTH

CEILING 1000 TO 5000 FEET INCLUSIVE  
 AND VISIBILITY 3 MILES OR GREATER

VISIBILITIES OVER 6 MILES NOT PLOTTED



MEAN REL. HUM. V.T. 0 HRS AFTER 00Z 19/2/72

Figure 6(B)

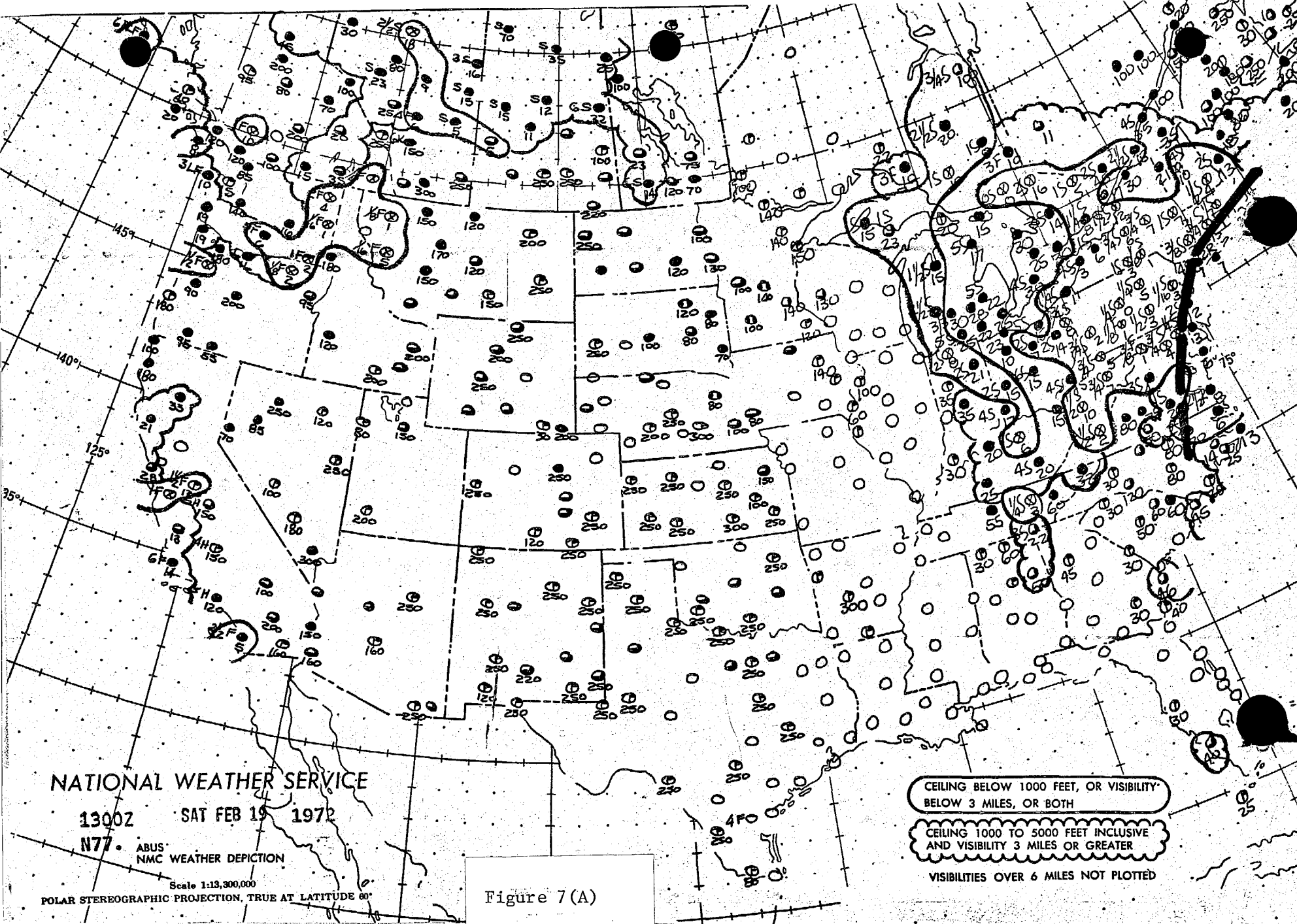
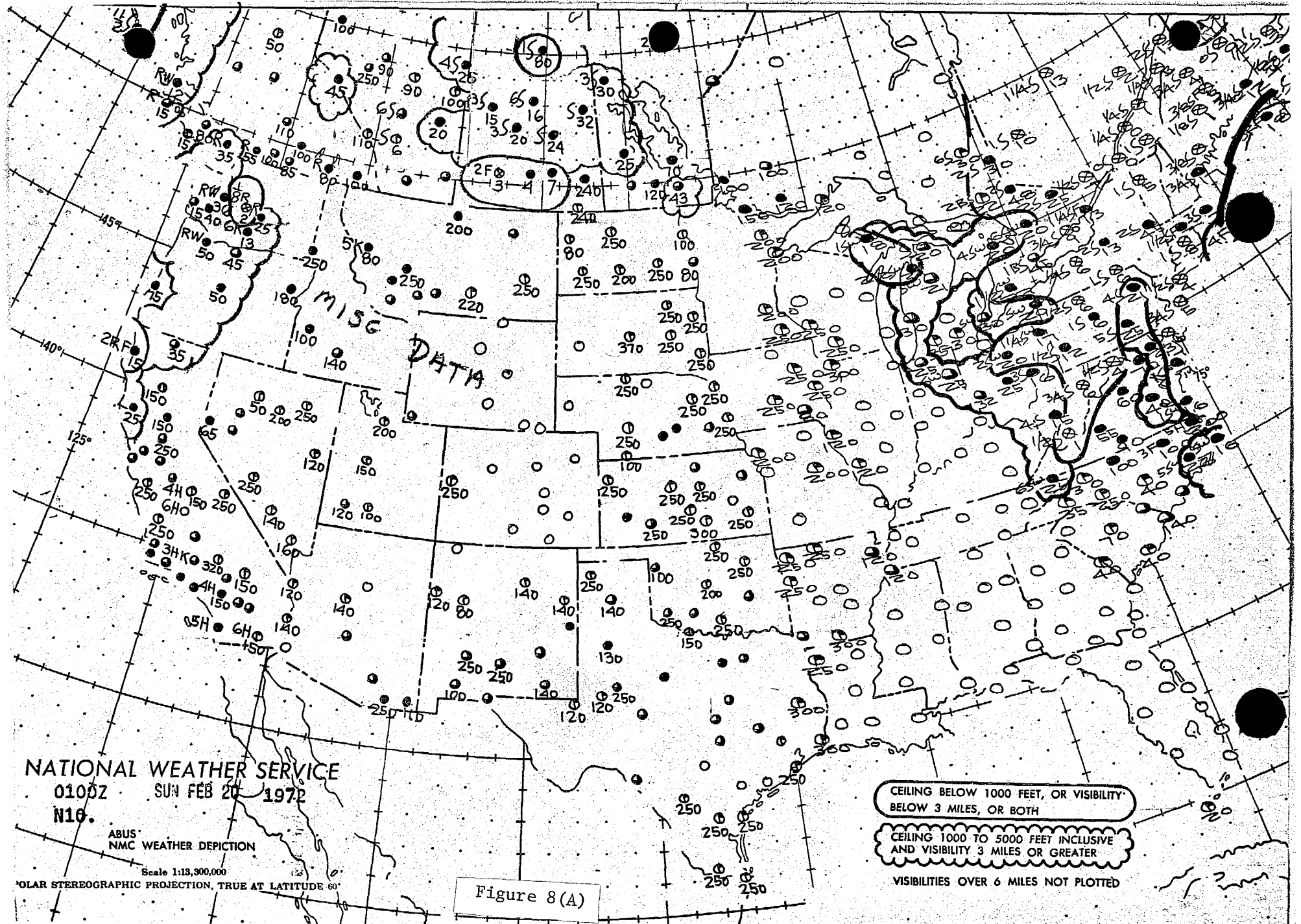


Figure 7(A)



NATIONAL WEATHER SERVICE  
 0100Z SUN FEB 20 1972  
 N10.

ABUS  
 NMC WEATHER DEPICTION

Scale 1:13,300,000

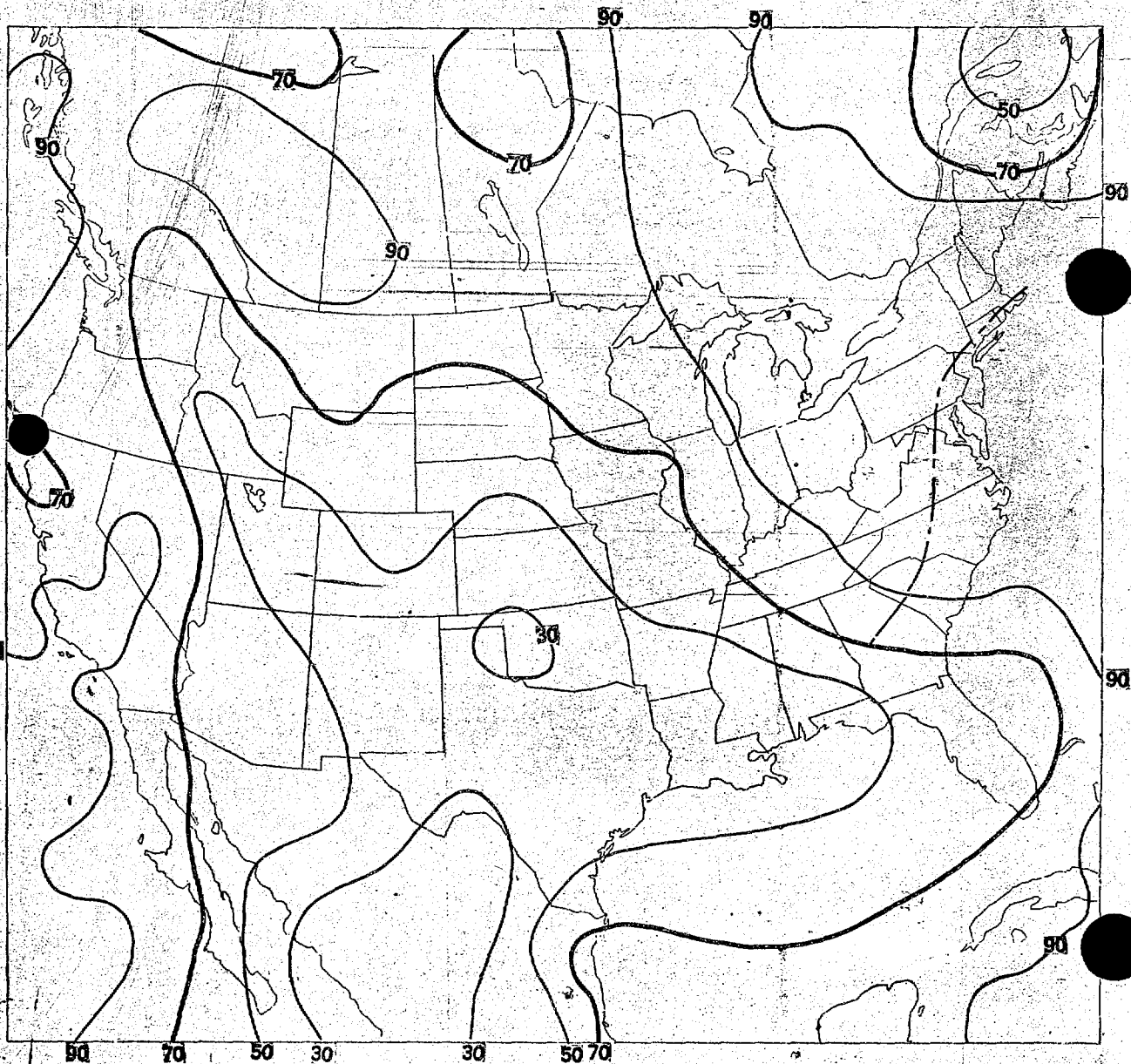
POLAR STEREOGRAPHIC PROJECTION, TRUE AT LATITUDE 60°

Figure 8(A)

CEILING BELOW 1000 FEET, OR VISIBILITY  
 BELOW 3 MILES, OR BOTH

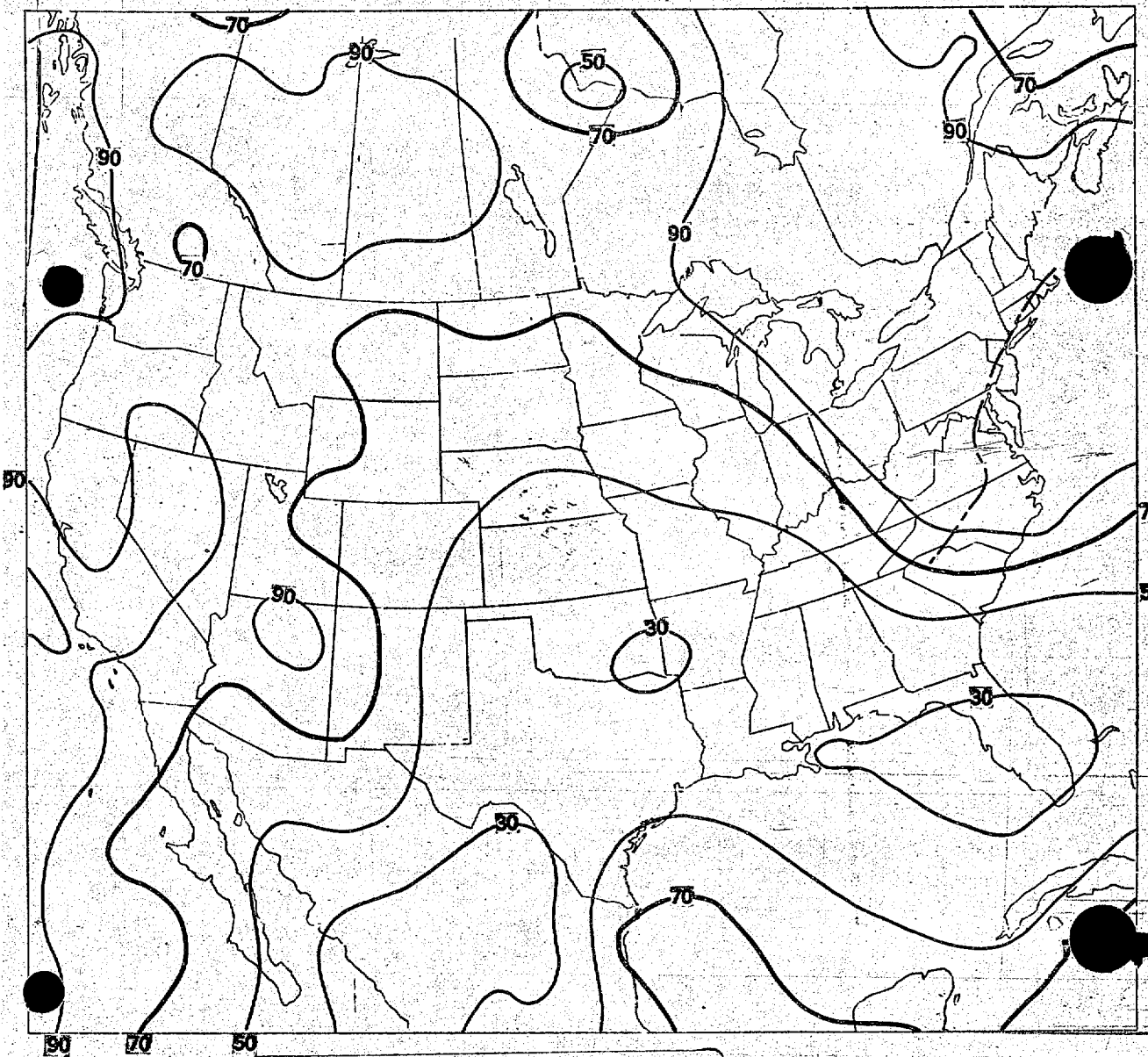
CEILING 1000 TO 5000 FEET INCLUSIVE  
 AND VISIBILITY 3 MILES OR GREATER

VISIBILITIES OVER 6 MILES NOT PLOTTED



MEAN REL. HUM. V.T. 12 HRS AFTER 00Z 19/2/72

Figure 7(B)

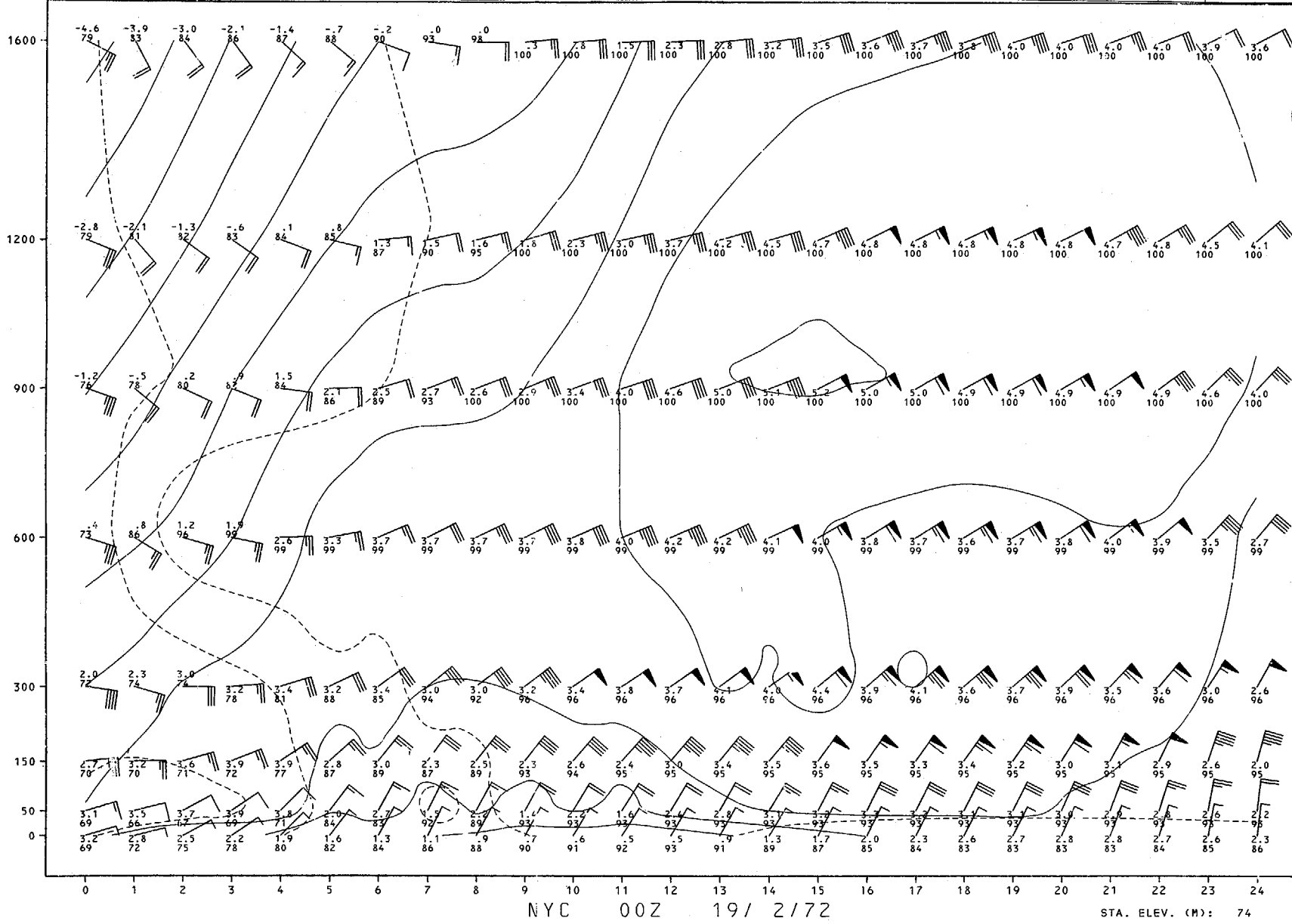


MEAN REL. HUM. V.T. 24 HRS AFTER 00Z 19/2/72

Figure 8(B)



N4C	M190	M200	M150	M140	M110	M60	W4K	W3K	W3Y	M100	M100	M100	E100	A100	80M100	M00	M40	M70	M70	M70	M50	70M120	W6X	-X100
WIND	0818	0817	0818	0718	0720	0516	0516	0619	0522	0525	0525	0618	0627	0524	0528	0424	0424	0622	0522	0619	0612	0321	3622	3421
TF	40°	40	40	40	39	36	35	35	35	35	36	37	38	39	39	41	41	40	39	38	36	36	32	32



SFC TEMP (°F)	37.8	37.1	36.4	35.9	35.4	34.9	34.4	33.9	33.5	33.2	33.0	32.9	32.8	33.6	34.3	35.0	35.7	36.2	36.6	36.9	37.1	37.1	36.9	36.6	36.2
---------------	------	------	------	------	------	------	------	------	------	------	------	------	------	------	------	------	------	------	------	------	------	------	------	------	------

Figure 10

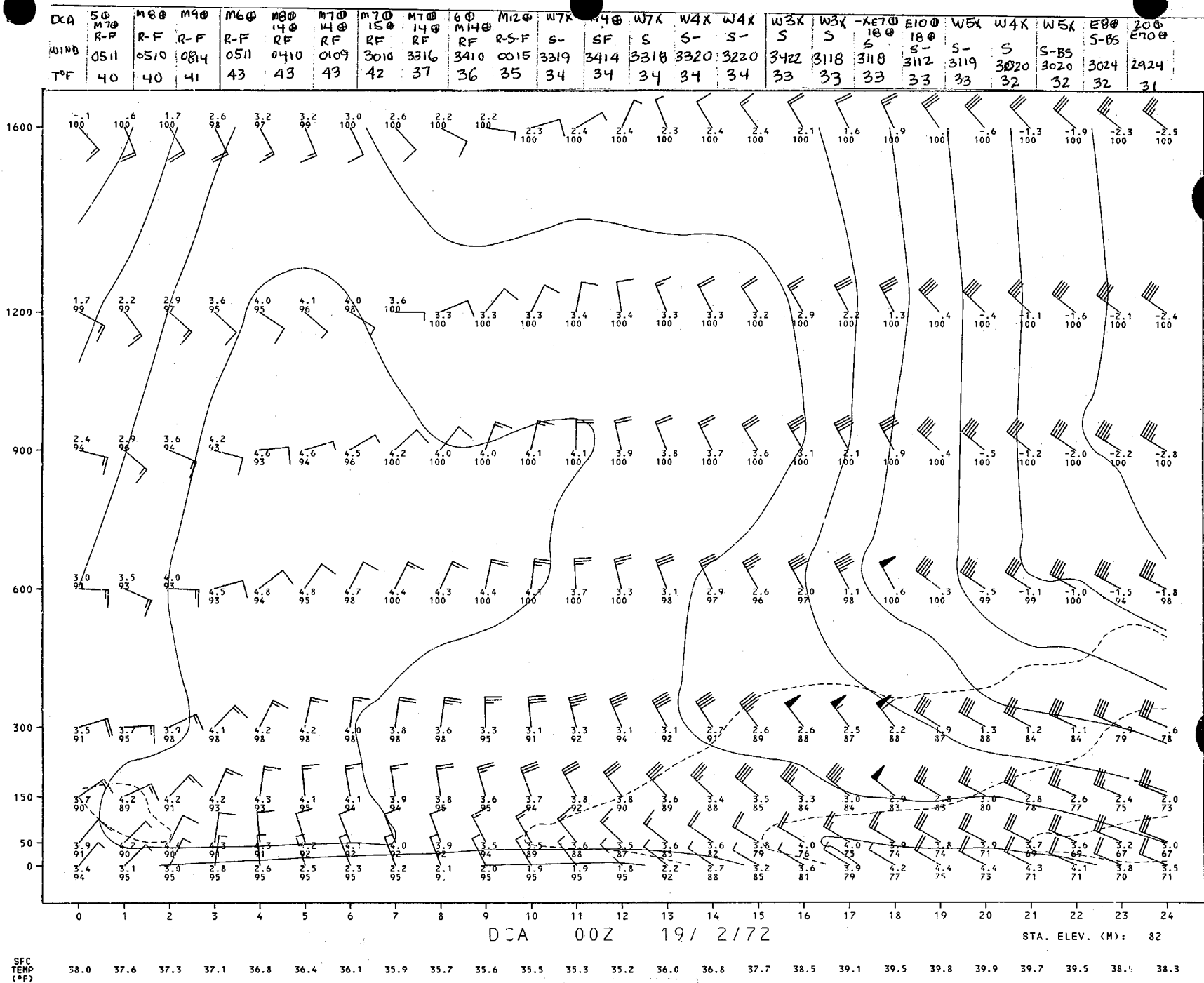
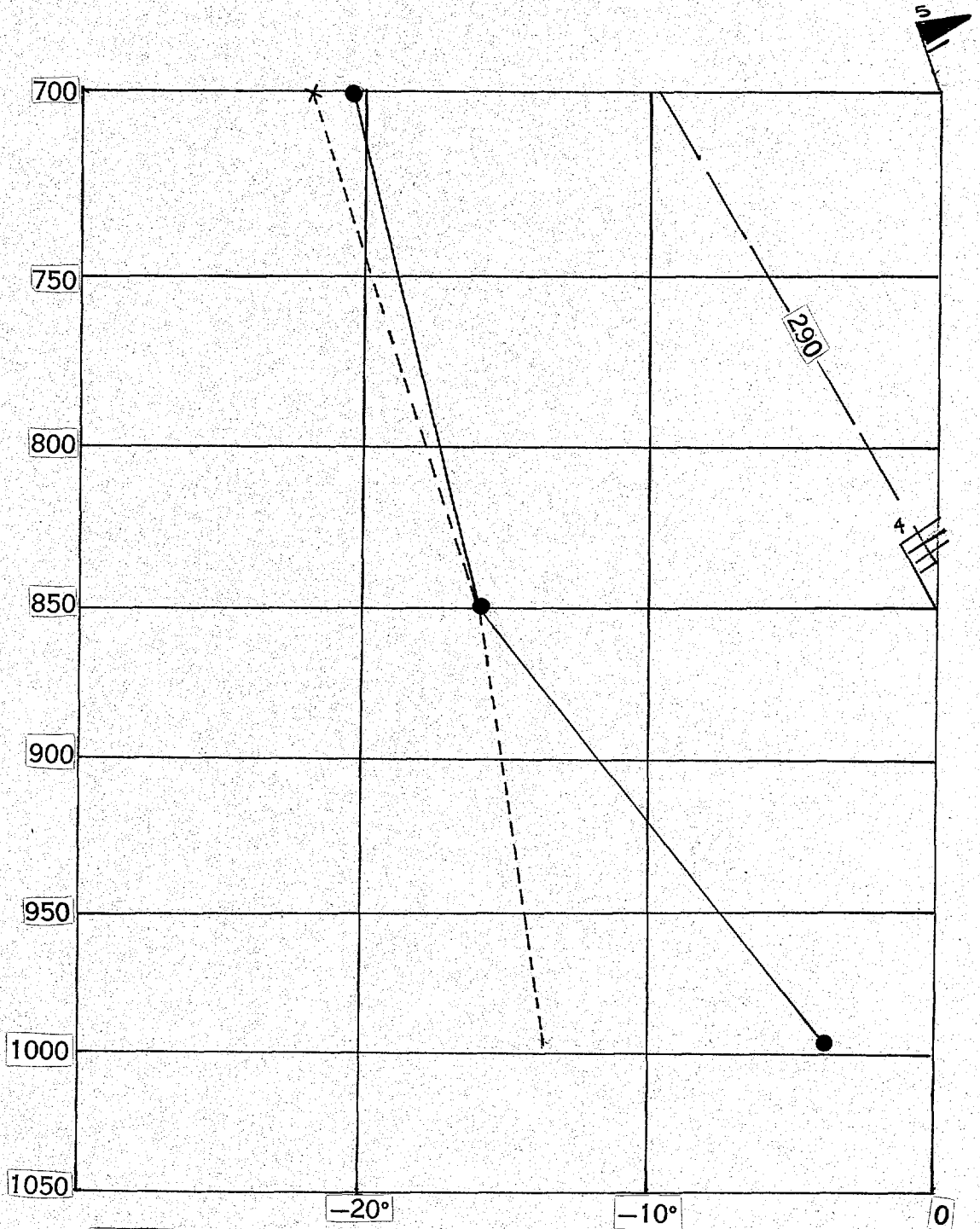
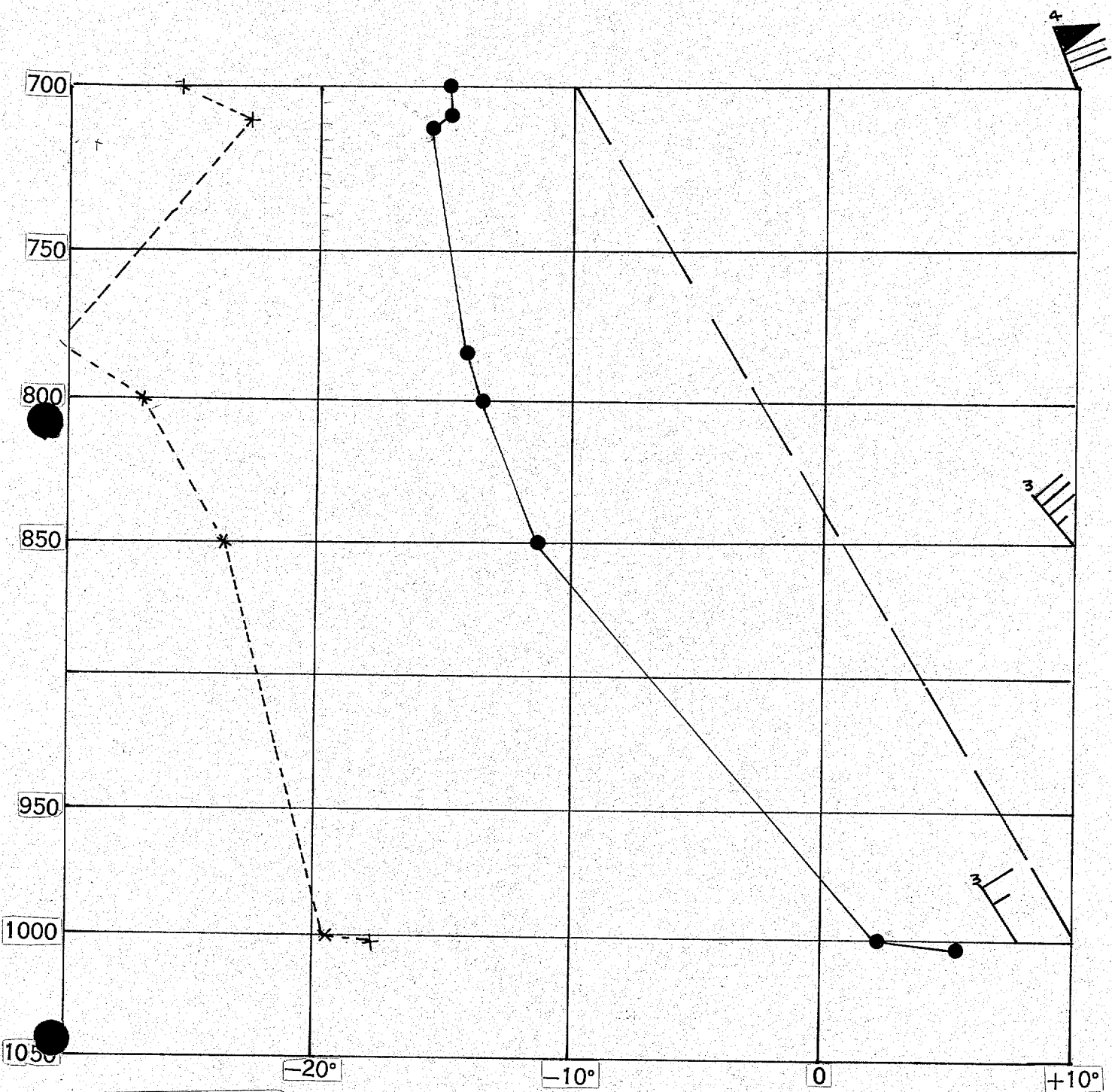


Figure 11



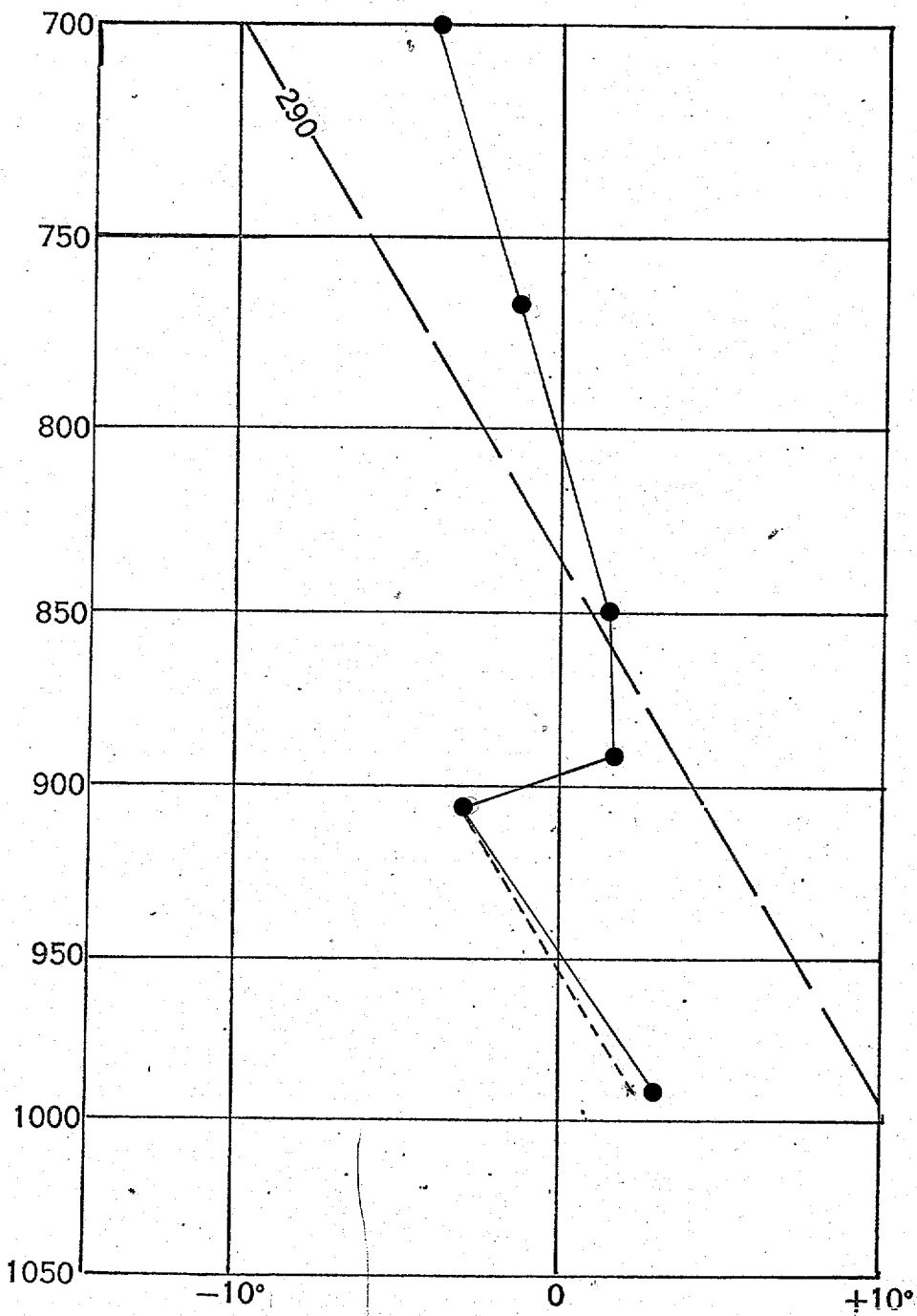
BNA  
1200Z 19 FEB 72

Figure 12(A)



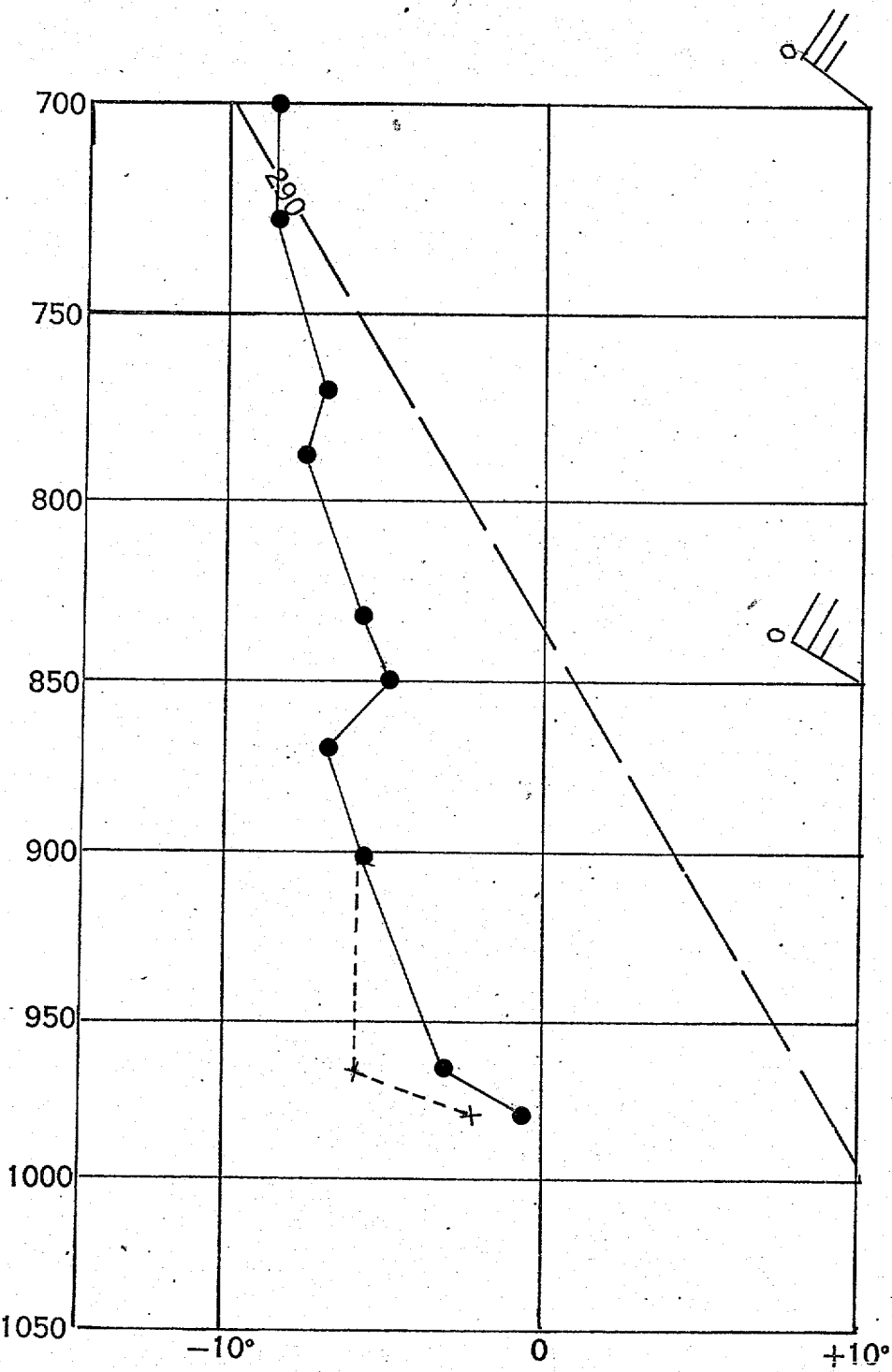
BNA  
0000Z 20 FEB 72

Figure 12(B)



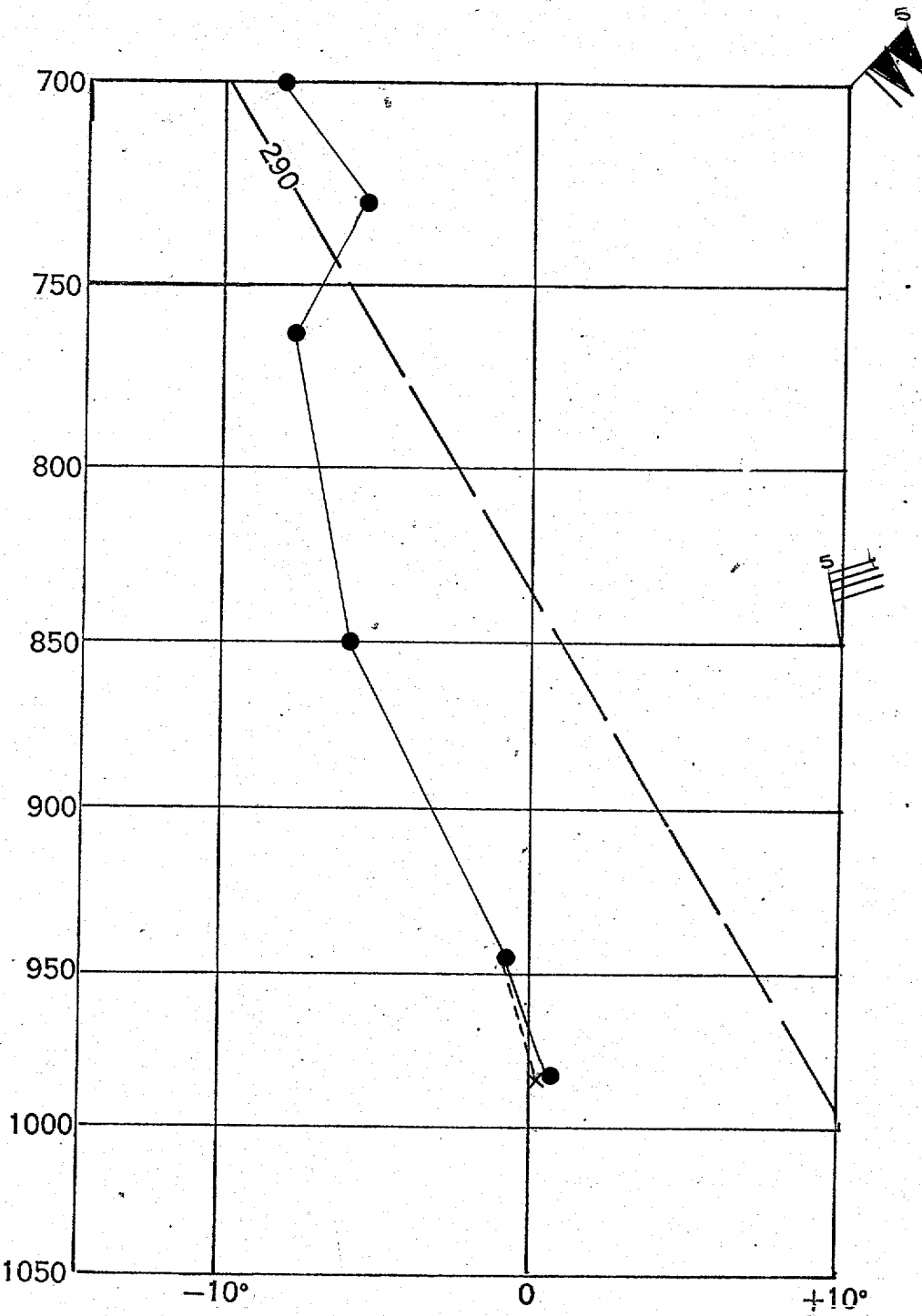
JFK  
1200Z 19 FEB 72

Figure 13(A)



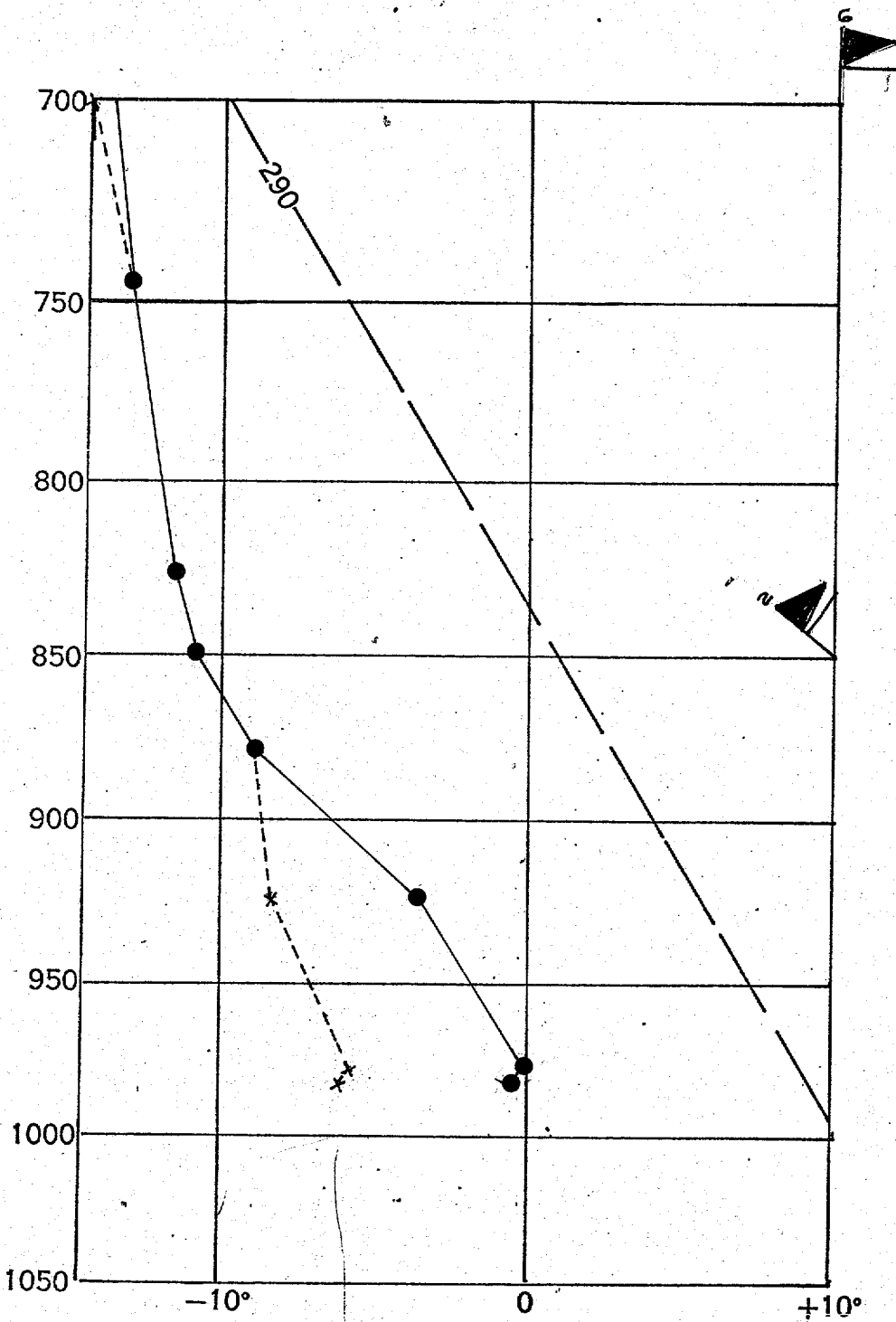
JFK  
0000Z 20 FEB 72

Figure 13(B)



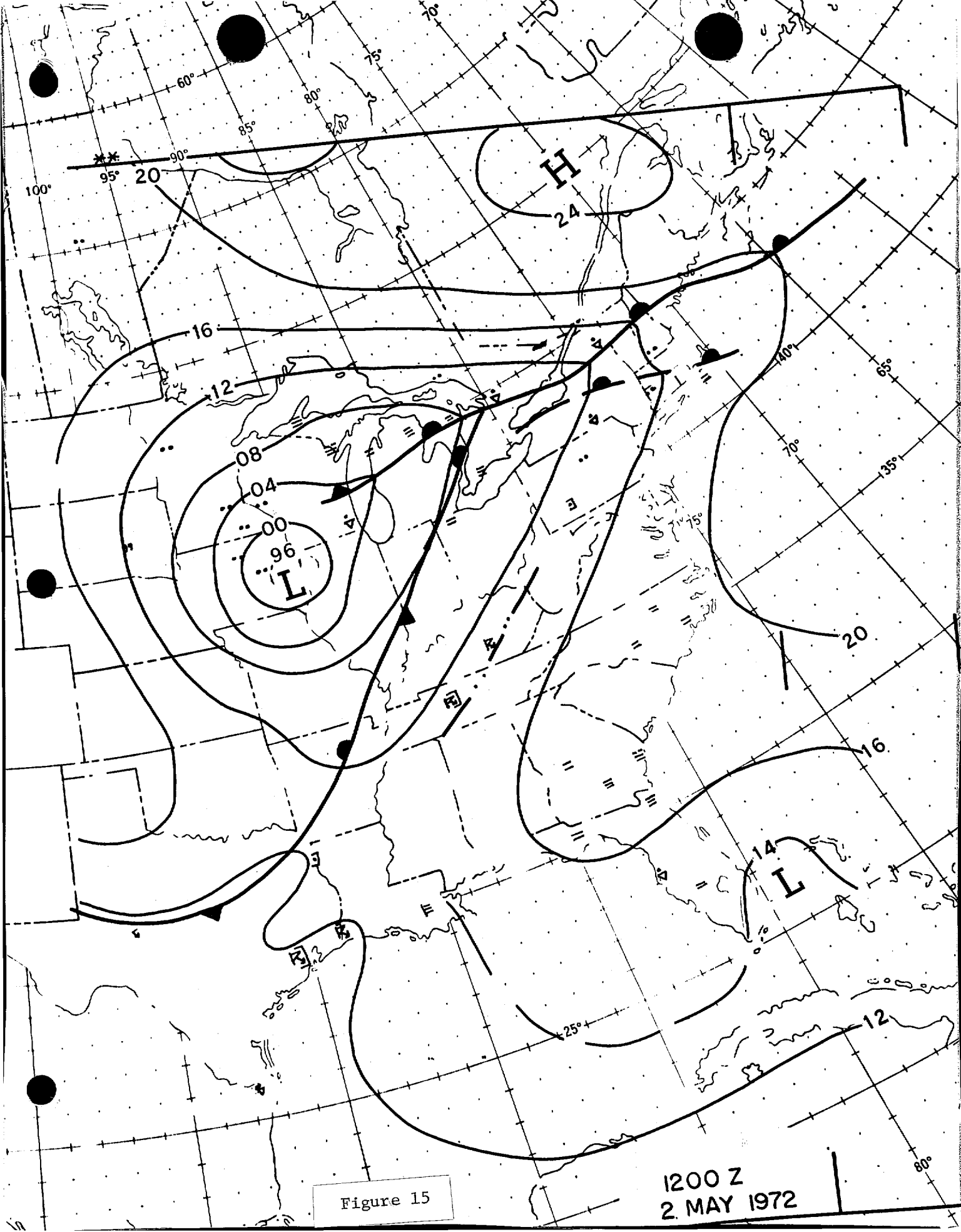
DTA  
1200Z 19 FEB 72

Figure 14(A)



DIA  
0000Z 20 FEB 72

Figure 14(B)





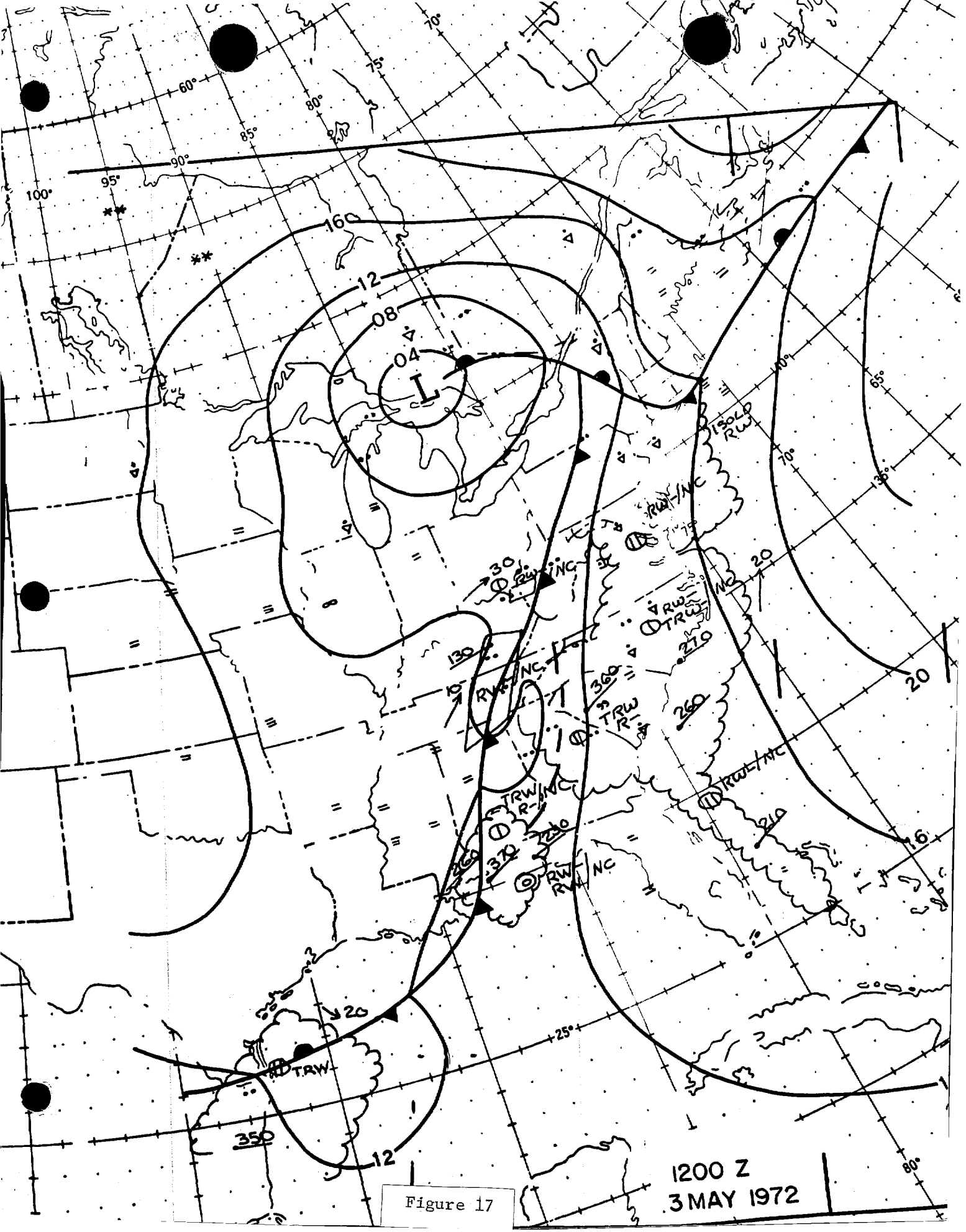
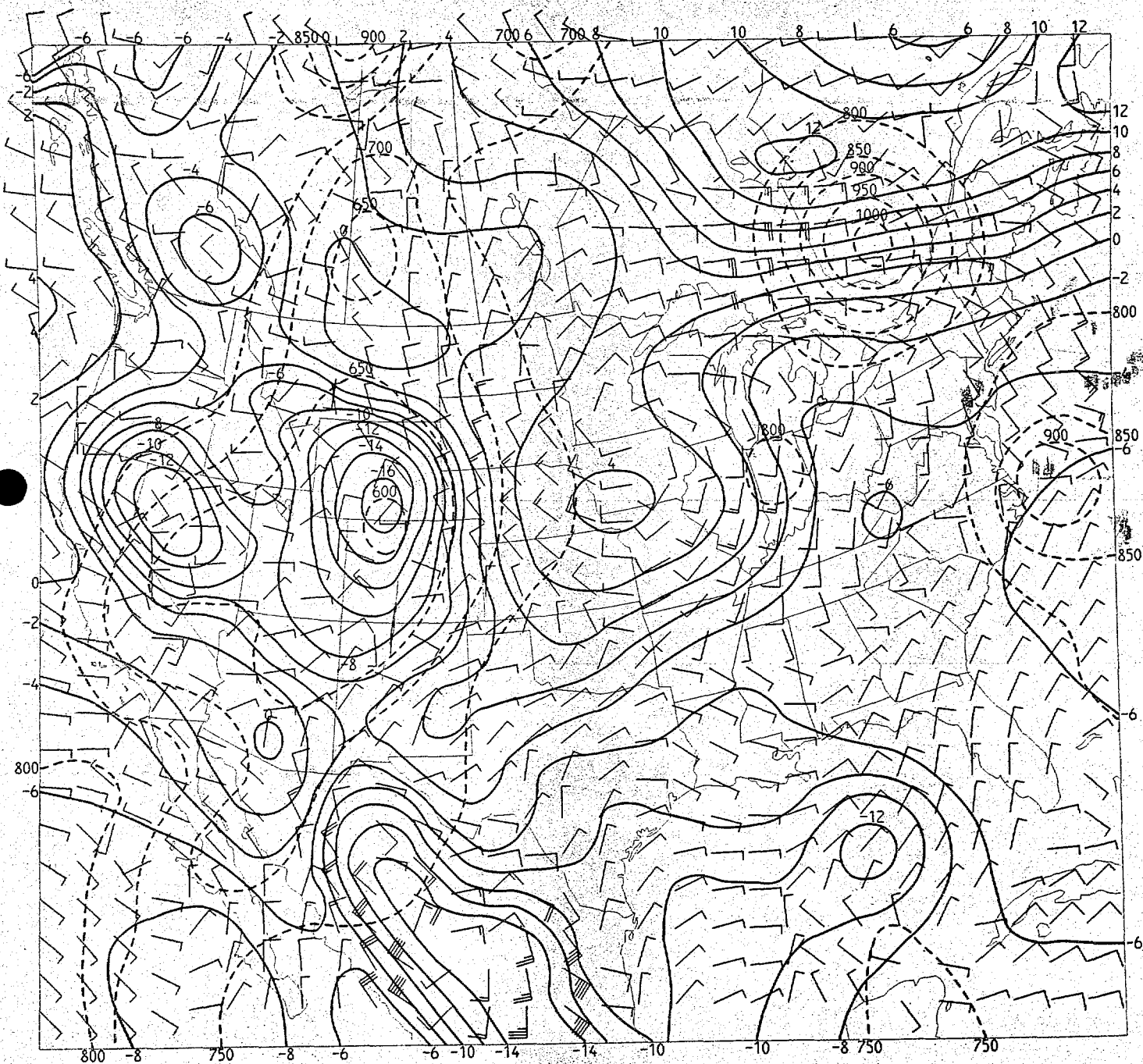


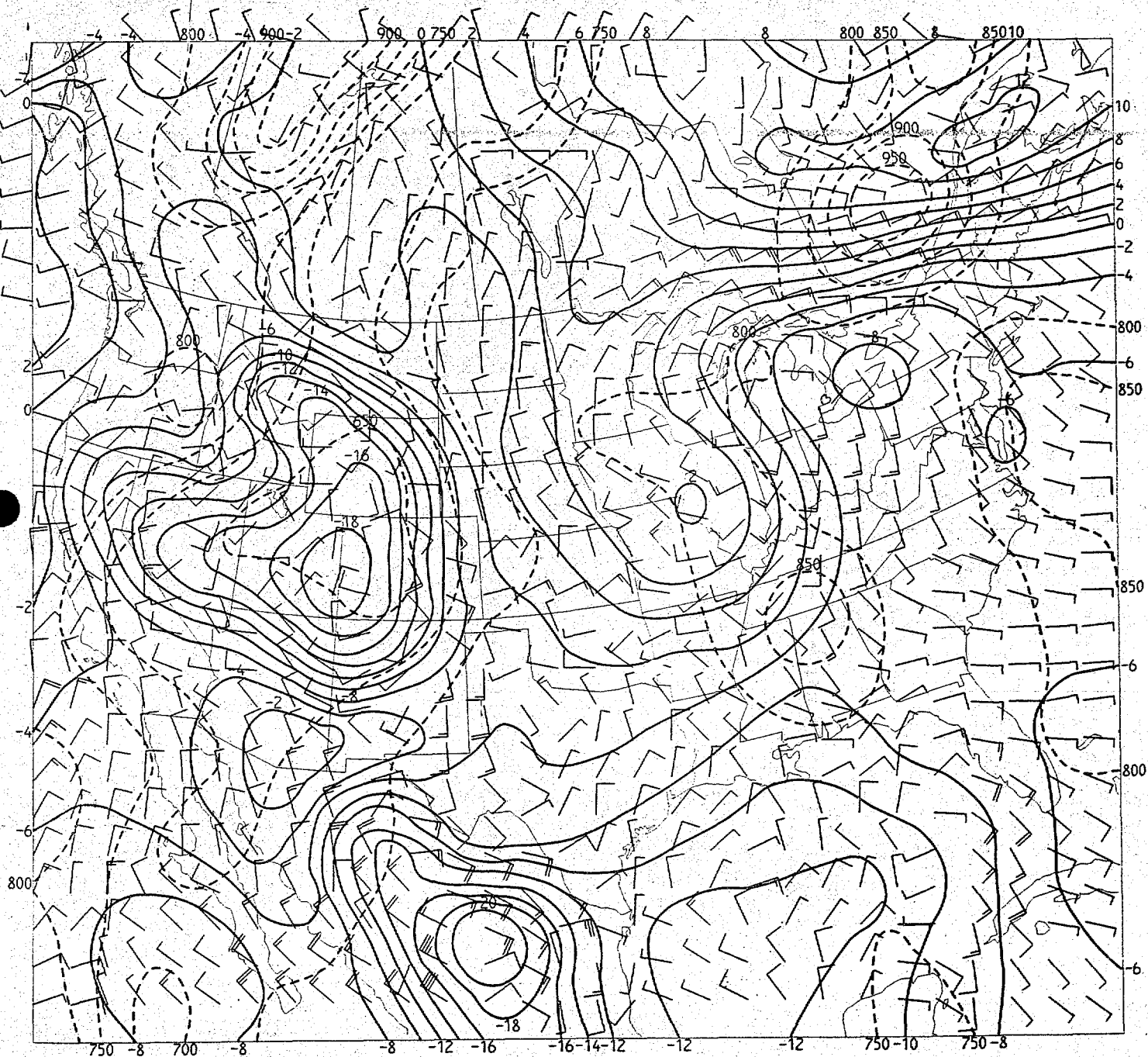
Figure 17

1200 Z  
3 MAY 1972



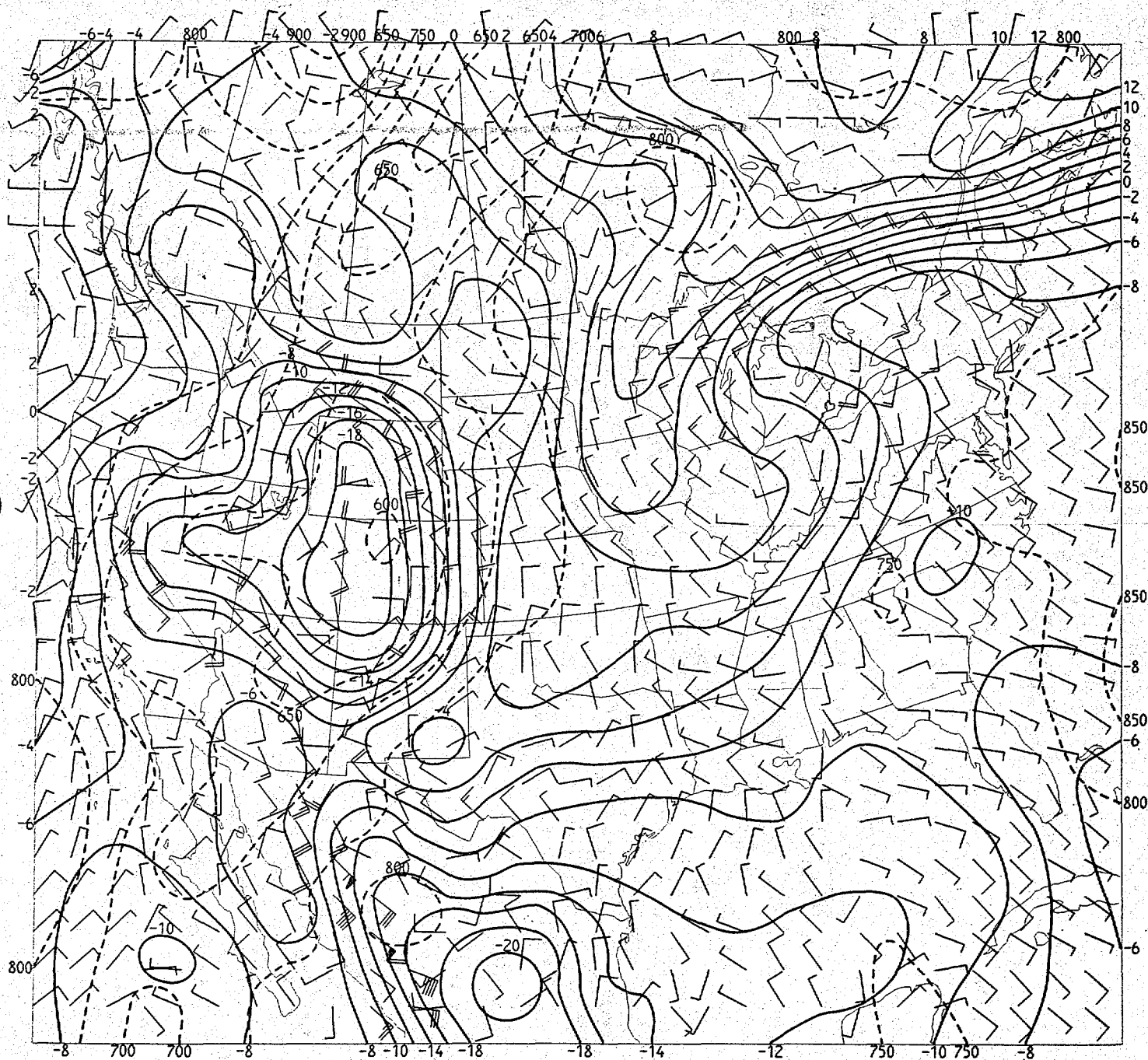
BEST LIFTED INDEX AND PRESSURE BLI V.T. 0 HRS AFTER 12Z 21 5/72

Figure 18



BEST LIFTED INDEX AND PRESSURE BLI V.T. 12 HRS AFTER 12Z 21/5/72

Figure 19



BEST LIFTED INDEX AND PRESSURE BLI V.T. 24 HRS AFTER 12Z 21 5/72

Figure 20